Calculation of the hyperfine splitting constants for the ground and excited states of NH_2 radical

H. Nakatsuji
Department of Synthetic Chemistry, Faculty of Engineering, Kyoto University and Institute for Fundamental Chemistry, Nishi-Hiraki-cho, Kyoto 606, Japan

M. Izawa
Production Engineering Research Laboratory, Hitachi Ltd., Totsukaku, Yokohama 244, Japan

(Received 20 February 1992; accepted 16 March 1992)

Hyperfine splitting constants of the ground $^2B_1$ and excited $^2A_1$ states of NH_2 radical are calculated by the symmetry adapted cluster-configuration interaction method with the use of the basis set which satisfies the cusp condition at the position of the nucleus. The calculated values compare well with the experimental values when the vibrational effects are considered for the $^2A_1$ state. The nature of the vibrational wave functions for the double well $^2A_1$ potential is discussed in some detail.

I. INTRODUCTION

Fermi contact hyperfine splitting constants (hfsc's) observed by electron-spin resonance (ESR) and microwave spectroscopy give information on the spin densities at the nuclei of an open shell molecule. Some experimental data of the hfsc's of short-lived electronic excited states have appeared with recent development of spectroscopic techniques. However, up to this time, most theoretical studies of Fermi contact hfsc's have been carried out only for the ground states.

The hfsc's of NH_2 and PH_2 in the electronic excited states have been observed by microwave spectroscopy.[1,2] For NH_2, the hfsc's were reported for both ground $^2B_1$ and first excited $^2A_1$ states, and those in the excited state were observed for high vibrational states ($n = 9,10$).[1] Theoretical investigation for the vibrational states were reported by Buenker *et al.*[3] In this paper, we study the Fermi contact hfsc's of NH_2 doublet radical in both $^2B_1$ and $^2A_1$ states.

As written in our previous paper,[4] three important factors must be considered for adequate descriptions of hfsc's: (1) spin polarization correction,[5-7] (2) electron correlation correction,[8-11] and (3) cusp condition[12] at the position of nuclei.[4,13,14] These factors are rather poorly described by the conventional *ab initio* molecular orbital methods.[6,15] Symmetry adapted cluster-configuration interaction (SAC-CI) theory[16,17] has been shown to be effective for describing both spin polarization and electron correlation corrections.[8] Since this method is very efficient, we can avoid configuration selection. Further, we have shown that the cusp condition is easily taken into account using the idea of the STO (Slater-type orbital)-GTO (Gaussian-type orbital) expansion.[4] Namely, the self-consistent field theory (SCF) and SAC-CI wave functions are calculated by using the GTO expansion of the STO's and the hfsc's and the cusp values are calculated using the original STO's. In the present paper, we use this method for calculating the potential energy and the nitrogen and proton hfsc's for the ground $^2B_1$ and excited $^2A_1$ states of NH_2 radical. We calculate the vibrational wave functions for the double well potential of the $^2A_1$ state and show the importance of the vibrational effect for the hfsc's of the higher vibrational states of the $^2A_1$ state.

II. METHOD

We have examined, in our previous paper,[4] the quality of several STO basis sets for calculating hfsc's. We use here the basis sets which were recommended previously: for nitrogen, we use the (5*s*) STO set of Bagus and Gilbert[18] and (5*p*)/[2*p*] contracted GTO for nitrogen[19] and for hydrogen, two 1*s* STO's ($\zeta = 1.0, 0.5$), 2*s* STO ($\zeta = 0.5$) plus *p* type GTO ($\zeta = 1.0$) polarization function. We use the STO's only for the *s* type AO's, since the cusp values are dependent essentially only on the *s* type AO's. We replace the above STO's by the GTO's using the STO 6G expansion of Stewart[20] when we calculate the integrals necessary for the SCF and SAC-CI wave functions. After obtaining the wave functions, we calculate the hfsc's and the cusp values using the original STO's. The computer programs which we have used are GAMESS[21] and SAC85[22] for the SCF and SAC-CI calculations, respectively.

In order to construct the electronic wave function of NH_2, we first calculate the SAC wave function using the SCF orbitals for the closed-shell anion NH_2^-. Then we construct the doublet B_1 and A_1 wave functions of NH_2 using ionization operators in the SAC-CI formalism. In the SAC step, we have performed configuration selection using the threshold $\lambda g = 10^{-5}$ a.u., (Ref. 23) but in the SAC-CI step, we have avoided it because spin densities are rather sensitive to this procedure.[8]

We use the geometry given by Jungen, Hallin, and Merer.[24] The N–H distance and the HNH angle are 1.034 Å and 102.4 deg for the $^2B_1$ state and 1.007 Å and 144.2 deg for the $^2A_1$ state. For the $^2A_1$ state, the effect of molecular vibration is taken into account using the following simple method. We calculate the bending vibrational wave function $\Psi_n(\theta)$, *n* being the vibrational quantum number, as a function of the valence angle θ alone, with fixing the N–H distance. We use the Fourier grid Hamiltonian method of Marston and Balint-Kurti[25] for solving the one-dimensional Schrödinger

 0021-9606/92/130435-05$06.00

TABLE I. Hyperfine splitting constants (Gauss), cusp values, and excitation energies (eV) at the equilibrium geometries of the $^2B_1$ (ground) and $^2A_1$ (first excited) states of NH_2 radical calculated by the SAC–CI method.

		Cusp Value		hfsc		Excitation energy[b]	
State	Nucleus	Calc.	Exact	Calc.	Expt.[a]	Calc.	Expt.[c]
$^2B_1$ (ground)	N	−14.12	−14.0	7.27	9.95		
	H	−2.32	−2.0	−20.12	−24.12		
$^2A_1$ (excited)	N	−14.12	−14.0	40.05	55.17 ($n=9$), 54.59 ($n=10$)	1.360	1.379
	H	−2.39	−2.0	8.72	17.63 ($n=9$), 18.63 ($n=10$)	(2.200)	

[a] Reference 1, the experimental hfsc's for the $^2A_1$ excited state are for the vibrational states with the quantum number $n=9$ and 10.
[b] Nonvertical excitation energy. Value in parentheses shows vertical excitation energy.
[c] Reference 24.

equation. The potential function in the vibrational Hamiltonian is calculated by the SAC-CI method. Although the vibrational coupling effect between the $^2A_1$ and $^2B_1$ states has some importance for the description of this system, as reported by Dixon[26] and Buenker *et al.*,[3] we neglect the contribution of the $^2B_1$ state and calculate the vibrational wave functions from the potential energy curve of the $^2A_1$ state alone. The reduced mass of NH_2 is fixed to that at $\theta = 145.15$ deg, which is the SAC-CI optimized angle, at any valence angle of NH_2, since its dependence on θ is very small. Then the expectation value of the hfsc of the nucleus B for the vibrational level n, $a_B(n)$, is given by[27]

$$a_B(n) = \langle \Psi_n(\theta) | a_B(\theta) | \Psi_n(\theta) \rangle, \qquad (1)$$

where $a_B(\theta)$ is the dependence of the hfsc of the $^2A_1$ state on the valence angle θ and is calculated by the SAC-CI method.

III. RESULTS AND DISCUSSIONS

Table I gives the results for the $^2B_1$ and $^2A_1$ states of NH_2 at their equilibrium geometries. The cusp values are slightly larger than the exact values, but the agreement is good. If we use the GTO's, these cusp values are essentially zero in quite a large disagreement with the exact values. The calculated hfsc's of the $^2B_1$ ground state compare well with the experimental values. However, those of the $^2A_1$ excited state are in disagreement, especially, for proton; the calculated value is less than a half of the experimental value. A reason for this disagreement is that the experimental values for the $^2A_1$ state were observed for the high vibrational states ($n = 9, 10$).[1] If the hfsc's of the $^2A_1$ state are strongly dependent on the bending angle, the vibrational averaging for the high vibrational states may give values different from those at the equilibrium geometry. The (nonvertical) excitation energy calculated by the SAC-CI method fairly agrees with the experimental value,[24] in accordance with our experiences.[28]

We next calculate the hfsc's of the first excited $^2A_1$ state, considering the effect of the molecular vibration. We first calculate the potential energy curve and the vibrational wave functions. Figure 1 shows the potential curve for the valence angle θ. It is a typical double well potential and is fitted by the 16th degree polynomial. The minimum is obtained at the valence angle of 145 deg which compares well with the experimental value 144 deg.[24,29] The barrier height is calculated to be 569 cm^{-1} which is smaller by about 160 cm^{-1} than the empirically fitted value 730 cm^{-1} (Ref. 24). The Renner–Teller effect is described well by the present electronic wave function.

The vibrational wave functions are calculated by numerically solving the one-dimensional Schrödinger equation for the potential given by Fig. 1. The calculated vibrational energy levels are given in Table II for the vibrational levels below $n = 20$, n being the vibrational quantum number. The first twelve levels are drown in Fig. 1. Reflecting the shallow double minimum shape of the potential curve, the level spacing is very small for the lower states, but increases as the state number increases. Since the calculated barrier is 569 cm^{-1}, only the first two states are below the barrier. This is in accordance with the result of Jungen *et al.*[24]

The energy levels for the $\Sigma(0,9,0)$ and $\Pi(0,10,0)$ states

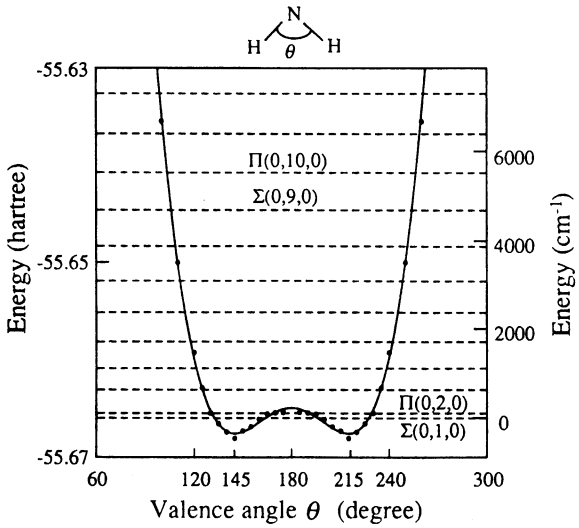

FIG. 1. Potential energy curve and the vibrational energy levels for the $^2A_1$ state of NH_2 radical. The energy levels are shown by the broken line.

TABLE II. Energy and hyperfine splitting constant (hfsc) for the vibrational state of the $^2A_1$ state of NH_2.[a]

State n	Energy (cm^{-1}) E_n	$E_n - E_{n-1}$	hfsc(Gauss) N	H
1	0	···	30.08	− 3.73
2	110	110	36.73	3.67
3	639	530	32.40	− 1.94
4	1 120	481	39.32	5.34
5	1 723	602	42.05	7.73
6	2 386	663	45.03	10.37
7	3 106	720	47.58	12.50
8	3 874	768	49.93	14.38
9	4 684	810	52.12	16.07
10	5 532	848	54.18	17.60
11	6 414	882	56.14	19.01
12	7 327	913	58.02	20.32
13	8 268	941	59.84	21.55
14	9 236	968	61.61	22.72
15	10 228	992	63.34	23.84
16	11 242	1014	65.04	24.91
17	12 277	1035	66.71	25.94
18	13 332	1055	68.36	26.94
19	14 406	1073	69.99	27.91
20	15 496	1090	71.61	28.85

[a] The barrier of the double well potential is calculated to be 569 cm^{-1}.

are calculated as 4684 cm^{-1} and 5532 cm^{-1}, respectively, relative to the lowest vibrational level of the $^2A_1$ state. The values obtained from the empirical potential curve are 5627 and 6451 cm^{-1}, respectively.[24]

Figure 2 shows the square of the vibrational wave function calculated for the potential curve shown in Fig. 1. Reflecting the double minimum nature of the potential curve, the lowest two states, which are below the barrier, have two peaks at near the minimum of the double wells. Interestingly, the lowest state, which is a Σ state, has a considerable amplitude at $\theta = 180$ deg, which is just due to the quantum effect: There is no chance of existence in the classical mechanics. The second level is a Π state so that it has a node at $\theta = 180$ deg. The third level, which is the first state over the barrier by 70 cm^{-1}, has a maximum peak at $\theta = 180$ deg. The number of peaks is equal to the vibrational quantum number n. The odd state is Σ and the even one Π. For the states $n = 4$ and 5, the peaks around $\theta = 180$ deg are still the highest, but for the states higher than $n = 6$, the highest peaks are the outermost peaks. For the states $n = 9$ and 10, for which the hfsc's are observed, the outermost peaks are considerably larger than the inner ones; as n increases, the picture approaches to the classical one. In comparison with the case of the harmonic osscilator,[30] the vibrational wave functions are quite different for the lower levels, but becomes similar as n increases. However, referring to Fig. 2, we see that the effect of the double well potential is seen even for the levels $n = 9$ and 10 as the peaks around $\theta = 180$ deg being larger than the neighboring peaks.

We next calculate the vibrational average of the hfsc's for the excited $^2A_1$ state using Eq. (1). Figures 3 and 4 show the hfsc's of the N and H nuclei, respectively, vs the valence

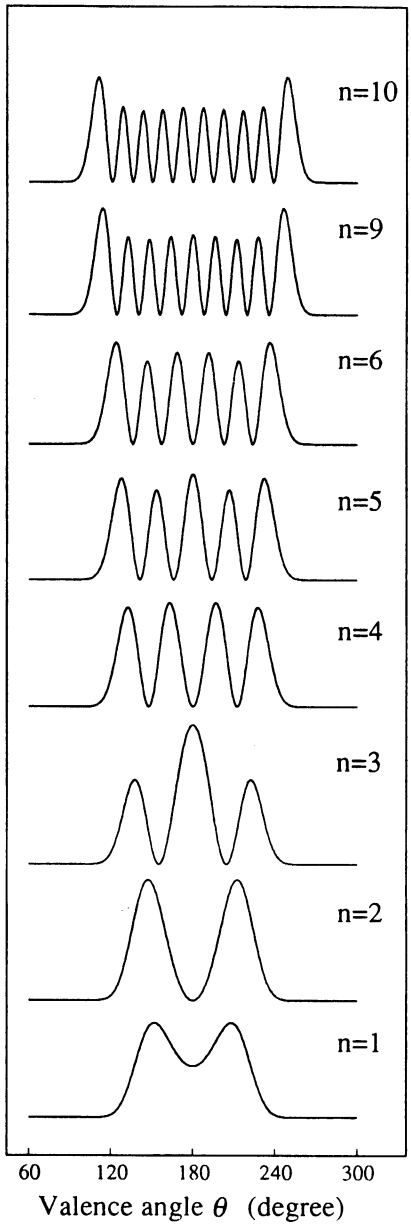

FIG. 2. Squares of the vibrational wave functions for the quantum numbers of $n = 1,2,3,4,5,6,9,10$ for the $^2A_1$ excited state of NH_2. They are normalized to unity.

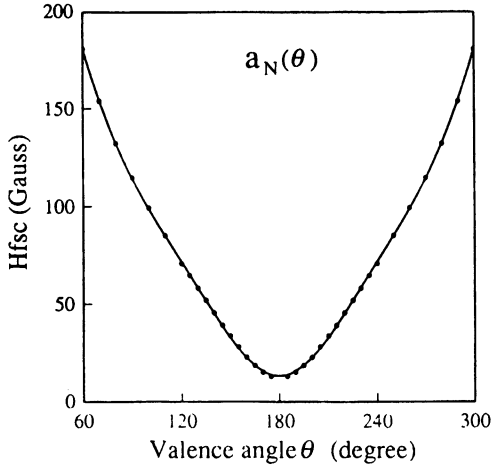

FIG. 3. Dependence of the calculated hyperfine splitting constant of the nitrogen atom on the valence HNH angle θ for the $^2A_1$ state of NH_2 radical.

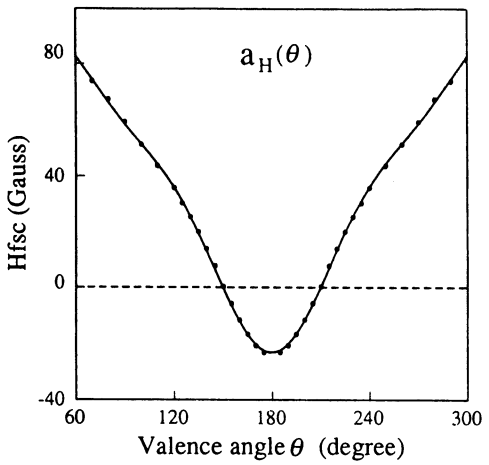

FIG. 4. Dependence of the calculated hyperfine splitting constant of the hydrogen atom on the valence HNH angle θ for the $^2A_1$ state of NH_2 radical.

angle θ for the $^2A_1$ state of NH_2. They are calculated by the SAC-CI method. Both of the nitrogen and proton hfsc's increase as the bending angle increases. The nitrogen hfsc is positive for all valence angles, but the proton hfsc is negative for the HNH angle larger than 150 deg, because at linear geometry the $^2A_1$ state becomes a π radical. We have fitted the hfsc curves shown in Figs. 3 and 4 by the 12th degree polynomials.

Table II gives the vibrational average of the hfsc's for the N and H nuclei for each vibrational level below $n = 20$. For the first three levels, the average values of a_N and a_H show interesting dependence on n. From $n = 1$ to 2, both a_N and a_H increase because of the increase of the outerside contribution, but from $n = 2$ to 3, the contribution around $\theta = 180$ deg increases as seen from Fig. 2, so that both a_N and a_H decrease. For the levels $n = 1$ and 3, a_H is negative because in these levels, there are considerable contributions of linear geometry. For the levels higher than $n = 3$, the hfsc's of both N and H monotonously increase. In comparison with the hfsc's calculated at the equilibrium geometry, $a_N = 40.05$ G and $a_H = 8.72$ G, the vibrational averages are smaller for the levels lower than $n = 4$ or 5. As the vibrational level increases, the probability amplitude increases in the outer region within the potential curve as shown in Fig. 2, so that as seen from Fig. 3 for $a_N(\theta)$ and Fig. 4 for $a_H(\theta)$, the vibrational averages of a_N and a_H increase.

Experimentally, the hfsc's of the first excited $^2A_1$ state of NH_2 were observed for the vibrational energy levels of $n = 9$ and 10. In Table III the calculated values of a_N and a_H for the vibrational levels $n = 9$ and 10 are compared with the experimental values. The agreement is excellent. For the proton hfsc, the ordering $a_H(n = 9) < a_H(n = 10)$ is obtained from both theory and experiment, but for a_N the ordering of the experimental values is $a_N(n = 9) > a_N(n = 10)$. This ordering of a_N is the one which is difficult for understanding from the present result alone. As seen from Table II, the vibrational averages of both a_H and a_N monotonously increase as n increases for the levels higher

TABLE III. Energy levels and the hyperfine splitting constants (hfsc's) including the vibrational effects for the excited $^2A_1$ state of NH_2.

Vibrational level n	a_N Calc.	a_N Expt.[a]	a_H Calc.	a_H Expt.[a]	Energy (cm^{-1}) Calc.	Energy (cm^{-1}) Empirical[b]
9	52.12	55.17	16.07	17.63	4684	5627
10	54.18	54.59	17.60	18.63	5532	6451

[a] Reference 1.
[b] Reference 24.

than $n = 4$, and this is a very reasonable result of the nature of the vibrational wave functions shown in Fig. 2 and the θ dependence of a_N and a_H shown in Figs. 3 and 4. The calculated energies for the vibrational levels $n = 9$ and 10 are smaller by about 1000 cm^{-1} than the values obtained from the empirical potential curve.[24]

A reason of the failure of reproducing the ordering $a_N(n = 9) > a_N(n = 10)$ may be the neglect of the orbit–rotation interaction. Hills *et al.*[1] suggested that the orbit–rotation interaction is larger for the state $n = 10$ which has Π symmetry than for the state $n = 9$ which has Σ symmetry. Since the orbit–rotation effect causes a mixing of the $^2B_1$ state into the $^2A_1$ state, the hfsc may decrease as a result. However, this argument does not explain why such ordering is observed only for a_N. Furthermore this effect should be larger for a_H than for a_N, since a_H of the $^2B_1$ state is a large negative as seen from Table I. Due to Hills *et al.*,[1] the experimental values are more reliable for the Π ($n = 10$) state than for the Σ ($n = 9$) state.

IV. CONCLUSION

The hfsc's for the ground $^2B_1$ and excited $^2A_1$ states of NH_2 are calculated by the SAC-CI method using the basis set which satisfies the cusp condition. For the ground state the SAC-CI results for the equilibrium geometry are in good agreement with the experimental values. For the hfsc's of the $^2A_1$ excited state, the observed values are for the high vibrational states, so that a reasonable agreement with the experimental values is obtained only after the inclusion of the vibrational effects which are fairly large for the hfsc's. The nature of the vibrational wave functions for the double well $^2A_1$ potential is discussed in some detail.

ACKNOWLEDGMENTS

The authers thank Dr. M. Hada at Kyoto University. The calculations have been carried out with the FACOM M780 computer at the Data Processing Center of Kyoto University and the HITAC M680 computer at Hitachi Production Engineering Research Laboratory. This study has partially been supported by the Grant-in-Aid for Scientific Research of HN.

[1] (a) G. W. Hills, C. R. Brazier, J. M. Brown, J. M. Cook, and R. F. Curl, J. Chem. Phys. **76**, 240 (1982); (b) G. W. Hills and J. M. Cook, J. Mol. Spectrosc. **94**, 456 (1982).

[2] M. Kakimoto and E. Hirota, J. Mol. Spectrosc. **94**, 173 (1982).
[3] R. J. Buenker, M. Peric, S. D. Peyerimhoff, and R. Marian, Mol. Phys. **43**, 987 (1981).
[4] H. Nakatsuji and M. Izawa, J. Chem. Phys. **91**, 6205 (1989).
[5] H. Nakatsuji and K. Hirao, Chem. Phys. Lett. **47**, 569 (1977); J. Chem. Phys. **68**, 4279 (1978); K. Ohta, H. Nakatsuji, K. Hirao, and T. Yonezawa, *ibid.* **73**, 1770 (1980).
[6] H. Nakatsuji, H. Kato, and T. Yonezawa, J. Chem. Phys. **51**, 3175 (1969).
[7] W. Meyer, J. Chem. Phys. **51**, 5149 (1969).
[8] H. Nakatsuji, K. Ohta, and T. Yonezawa, J. Phys. Chem. **87**, 3068 (1983); T. Momose, H. Nakatsuji, and T. Shida, J. Chem. Phys. **89**, 4185 (1988).
[9] S. Y. Chang, E. R. Davidson, and G. Vincow, J. Chem. Phys. **52**, 1740, 5596 (1970).
[10] D. Feller and E. R. Davidson, J. Chem. Phys. **80**, 1006 (1984); Theor. Chim. Acta **68**, 57 (1985).
[11] H. Sekino and R. J. Bartlett, J. Chem. Phys. **82**, 4225 (1985).
[12] T. Kato, Commun. Pure Appl. Math. **10**, 151 (1957).
[13] K. Ishida, Int. J. Quantum Chem. **28**, 349 (1985); **30**, 543 (1986).
[14] T. Momose and T. Shida, J. Chem. Phys. **87**, 2832 (1987).
[15] H. Nakatsuji, J. Chem. Phys. **59**, 2586 (1973).
[16] H. Nakatsuji, Chem. Phys. Lett. **59**, 362 (1978); **67**, 392, 334 (1979).
[17] H. Nakatsuji and K. Hirao, J. Chem. Phys. **68**, 2053 (1978).
[18] P. S. Bagus and T. L. Gilbert cited in A. D. McLean and M. Yoshimine, IBM J. Res. Dev. Suppl. **12**, 206 (1968).
[19] S. Huzinaga, J. Chem. Phys. **42**, 1293 (1965); T. H. Dunning, *ibid.* **53**, 2823 (1970).
[20] R. F. Stewart, J. Chem. Phys. **52**, 431 (1970).
[21] B. R. Brooks, P. Saxe, W. D. Laidig, and M. Dupuis, Program System GAMESS, Program Library No. 481, Computer Center of the Institute for Molecular Science, 1981.
[22] H. Nakatsuji, Program System for SAC and SAC-CI calculations, Program Library No. 146 (Y4/SAC), Data processing Center of Kyoto University, Kyoto, 1985; H. Nakatsuji, Program Library SAC85 (No. 1396), Computer Center of the Institute for Molecular Science, Okazaki, 1986.
[23] H. Nakatsuji, Chem. Phys. **75**, 425 (1983).
[24] C. Jungen, K-E. J. Hallin, and A. J. Merer, Mol. Phys. **40**, 25 (1980).
[25] C. C. Marston and G. G. Balint-Kurti, J. Chem. Phys. **91**, 3571 (1989).
[26] R. N. Dixon, Mol. Phys. **9**, 357 (1965).
[27] K. Ohta, H. Nakatsuji, I. Maeda, and T. Yonezawa, Chem. Phys. **67**, 49 (1982).
[28] H. Nakatsuji, Rep. Mol. Theory (in press).
[29] G. Herzberg, *Molecular Spectra and Molecular Structure*, Vol. III, *Electronic Spectra and Electronic Structure of Polyatomic Molecules* (Van Nostrand, Princeton, 1967).
[30] L. Pauling and E. B. Wilson, *Introduction to Quantum Mechanics* (McGraw-Hill, New York, 1935).